Journal of Bioinformatics and Computational Biology
Vol. 13, No. 2 (2015) 1550007 (20 pages)

DOI: 10.1142/S0219720015500079

Imperial College Press
www.icpress.co.uk

Validation of signalling pathways: Case study of the p16-mediated pathway

Nimet İlke Akçay[*,‡], Rza Bashirov[*,§] and Şükrü Tüzmen[†,¶]

[*]*Department of Applied Mathematics and Computer Science*
Eastern Mediterranean University
Famagusta, North Cyprus, Mersin-10, Turkey

[†]*Department of Biological Sciences*
Eastern Mediterranean University
Famagusta, North Cyprus, Mersin-10, Turkey
[‡]*ilke.cetin@emu.edu.tr*
[§]*rza.bashirov@emu.edu.tr*
[¶]*sukru.tuzmen@emu.edu.tr*

Received 18 July 2014
Revised 29 September 2014
Accepted 1 December 2014
Published 13 January 2015

p16 is recognized as a tumor suppressor gene due to the prevalence of its genetic inactivation in all types of human cancers. Additionally, p16 gene plays a critical role in controlling aging, regulating cellular senescence, detection and maintenance of DNA damage. The molecular mechanism behind these events involves p16-mediated signaling pathway (or p16-Rb pathway), the focus of our study. Understanding functional dependence between dynamic behavior of biological components involved in the p16-mediated pathway and aforesaid molecular-level events might suggest possible implications in the diagnosis, prognosis and treatment of human cancer. In the present work, we employ reverse-engineering approach to construct the most detailed computational model of p16-mediated pathway in higher eukaryotes. We implement experimental data from the literature to validate the model, and under various assumptions predict the dynamic behavior of p16 and other biological components by interpreting the simulation results. The quantitative model of p16-mediated pathway is created in a systematic manner in terms of Petri net technologies.

Keywords: Signaling pathway; p16-mediated pathway; hybrid functional Petri net; quantitative modeling.

1. Introduction

Achievements in molecular biology and genetics over the past few decades have created a tremendous gap between accumulated biological data and their interpretation. Bringing together *a posteriori* knowledge with mathematical formalism

[§]Corresponding author.

and tools of computer science provides an essential vehicle to close the existing gap. Computational modeling and simulation is a well-known approach to explore biological systems. The main idea behind this approach is to create the closest approximation of a biological system based on wet lab results, and predict its dynamic behavior through measuring the amounts of biological components. The success of this approach depends on success in all of its phases, which are the selection of appropriate modeling tool, gradual model development and its careful adjustment, model validation and prediction of dynamic behavior through simulation and analysis of simulation results. Researchers have come to realize that an appropriate modeling tool not only has to reproduce the biological system to desired outcome, but also allow us to predict its behavior by interpreting the simulation results in a meaningful way. Nowadays, there exists a consensus among researchers that a quantitative description of dynamic behavior is inevitable to fully understand biological systems with complex interacting components.

With the advent of The Human Genome Project, scientists announced that they have identified approximately 20,000–25,000 genes on the whole human genome. What we do know is that not all genes are equally important for survival of living organisms. Some genes are of critical importance, while others are of much less importance. The present research is focused on p16,[1,2] a crucial player orchestrating a prominent role in controlling DNA damage and tumor suppression,[3] replicative senescence and aging.[4,5] Furthermore, p16 plays an important role in cell cycle regulation,[6] particularly facilitating the regulation of p16-mediated signaling pathway. Inactivation of p16 leads to disruption of p16-mediated signaling pathway, a key cause of cancers in humans.[7,8] As part of the consensus of p16 utilization as a potential biomarker for detection and diagnosis of cancer, p16 immunohistochemistry is gaining significance.[9,10] Overall, this is the strongest argument to motivate further research in this area.

There exists a dozen of quantitative models describing various aspects of cell cycle regulation.[11–29] Several comprehensive reviews are available on existing mathematical and computational models.[30,31] Still, research on this field is far from over.[32] In particular the details of the inhibitory role of p16 in replicative senescence and DNA damage, as well as the relationship between the p16 mutations and their interaction with protein complexes remain largely unanswered. The present research, to the best of authors knowledge, describes the most detailed quantitative model of p16-mediated pathway in higher eukaryotes, incorporating the latest experimental observations. We study the quantitative changes in dynamic behavior of the major proteins and protein complexes in response to the mutations of p16 and G1-dysfunction. In this respect, it is noteworthy that our model gives insight into key role of p16 in regulation of replicative senescence and DNA damage. Throughout our modeling system, we compare the behavior of the major proteins with experimental data, to validate our model and assess in what measure the model reproduce the dynamics of p16-mediated pathway.

In the present research, we exploit hybrid functional Petri net (HFPN) as computational platform to create quantitative and explanatory model of p16-mediated pathway, describing the processes of the cell cycle regulation at G1 phase. We perform a series of simulations to validate the model for wild type p16 and its mutated form. Simulation results facilitate understanding of the dynamic behavior of p16 in a normal functioning cell as opposed to a dysfunctional cell when DNA damage or replicative senescence occurs.

The paper is organized as follows: We start with introducing the molecular mechanism behind p16-mediated signaling pathway to make it easy for the readers to understand the present research. Then we succinctly review Petri nets, from its simplest form to HFPN. After that, we present our HFPN model of p16-mediated pathway, and draw a connection between model components and biological content. Following this, we discuss the simulation results, and we summarize our findings.

2. The p16-Mediated Signaling Pathway

The tumor suppressor genes p16 and p21 play a key role in detection and repair of DNA damage and keeping track of replicative senescence. The p16 and p21 utilize their functions in G1 phase and G1/S checkpoint, respectively. Figure 1 is a schematic illustration of p16- and p21-mediated control mechanism occurring in human cells. In wild-type human cells, Cdk4 binds to Cdk6, which in turn activates cyclin D, and further inactivates Rb by phosphorylating it. Phosphorylation of Rb by Cdk4/6

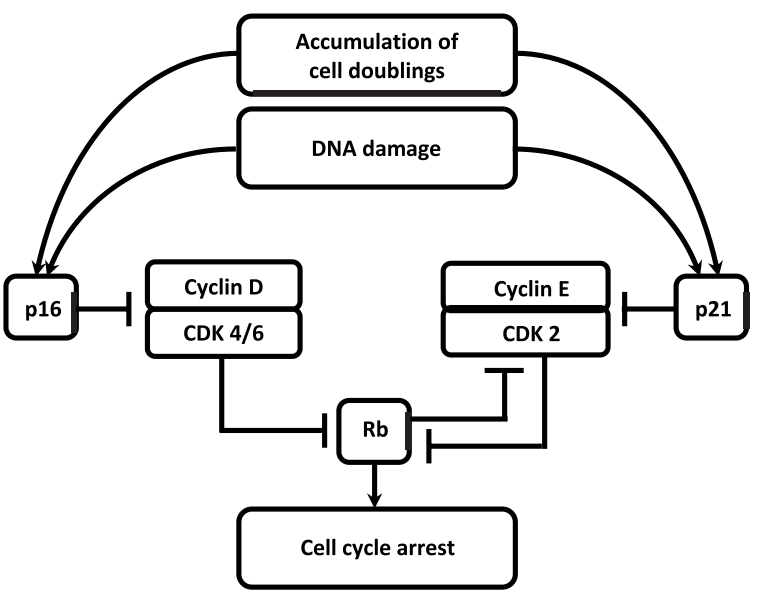

Fig. 1. Schematic illustration of p16- and p21-mediated control mechanism regulating DNA damage and replicative senescence.

leads to activation of cyclin E, which in turn forms a complex with Cdk2. A complex CycECdk2 further phosphorylates pRb. Phosphorylation of pRb by CycECdk2 inactivates it and allows cells to enter S phase, resulting in the initiation of DNA replication.[33,34] When number of accumulated cell doublings reaches the Hayflick limit[35] p16 receives a signal on replicative senescence. As a result p16 binds to Cdk4/6 inhibiting its activity thereby preventing Rb phosphorylation.[36,37] This leads to irreversible arrest in G1 phase of cell cycle. When DNA damage is detected, the action of p16 again targets Cdk4/6 and results in arrest in G1 phase until DNA damage is repaired. Inactivation of tumor suppressor gene p16 occurs through its mutation. Mutated p16 gene looses its gatekeeper role at G1 phase which might cause uncontrolled cell division leading to cancer.[38] When p16 is mutated, p21 takes responsibility for controlling its functions in G1/S checkpoint.

3. Petri Nets

A concept of Petri nets was introduced by Dr. Carl Adam Petri in 1962. An original Petri net sometimes referred to as P/T-net, is suitable for modeling discrete dynamic systems in which both systems states and transitions between the states are represented in terms of integers. In order to add more modeling power and match modeling tool to systems characteristics, P/T-net is sometimes expanded with time, color, hierarchy, stochasticity, fuzzibility, and other extensions. In a P/T-net with extension, a state is basically composed of discrete and boolean components.

Nevertheless, a P/T-net with extension is not suitable for modeling the dynamic systems with continuously changing state parameters. Continuous Petri nets were introduced to overcome this drawback.[39] In a continuous Petri net, real numbers are used to represent continuous change of state parameters. Many dynamic systems are however naturally hybrid employing different structured processes. A state in hybrid systems is a collection of integers, real numbers, boolean values, etc. Hybrid Petri nets are specifically developed to comprise different structured data types, and express explicitly the relationship between continuous and discrete values.[40]

Modeling of biological systems requires often interaction between different structured processes. Biological reactions are natural continuous processes. Reaction rate or reaction speed at which a biological reaction takes place is usually expressed in terms of real numbers. On the other hand, checking for presence/absence of biological phenomenon is a boolean process, while counter-like mechanism is a typical discrete process. In biological reactions, concentration of output component depends on concentrations of input components and the reaction rate. Reaction rates are determined in accordance with the functions that are assigned to biological processes. HFPN is inherited from hybrid Petri net in which a function is associated with each continuous process. HFPN has been successfully used for modeling and simulation of many biological processes.[41–44]

4. Model Construction

When modeling biological systems, the researchers use terms that are meaningful in biological context. We use terminology adopted in many articles,[42–44,59,60] and rename place, transition, arc and token respectively as entity, process, connector and quantity in compliance with the biological content. Our model is centered upon gatekeeper role of p16 in regulating p16-mediated pathway. Cascade of biological events induced by each of four possible scenarios regarding p16 mutation and G1-dysfunction are described in Fig. 2. We create HFPN model of p16-mediated pathway from biological content information that is discussed in the literature.[24,33–38,45,61–69] The present model is centered around interactions between four major proteins: p16, cyclin D, Cdk4 and Cdk6. We suppose that each major protein is synthesized in accordance with the central dogma of molecular biology. A protein is synthesized in the cytoplasm and then transported to the nucleus; and that the abundance of mRNA that no longer used for protein production as well as all unnecessary proteins and protein complexes are destroyed by degradation. Figure 4 exemplifies aforesaid biological phenomena for Cdk4. Our model incorporates similar net fragments for p16, cyclin D and Cdk6. In Fig. 5, we propose a skeleton model of the p16-mediated pathway. In this figure, for the sake of clarity we discard graphical description of protein syntheses and other satellite data discussed so far, and try to emphasize on molecular

		G1-DYSFUNCTION	
		YES	NO
P16 MUTATION	YES	❖ Mutated p16 loses its inhibitory function. ❖ If the reason of dysfunction is replicative senescence, cells evade replicative senescence, gaining immortality, or an extended replicative lifespan, which leads to tumor progression in an organism. ❖ If the reason of dysfunction is DNA damage, there is no way to arrest cellcycle at G1 phase and maintain damaged DNA. Damaged DNA results in loss of genetic information and mutations.	❖ Mutated p16 loses its inhibitory function. ❖ CycD binds to CDK4/6 resulting in phosphorylation of Rb, causing successive cell division until Hayflick limit is reached or DNA damage arises. ❖ When the Hayflick limit is reached, cells evade replicative senescence, gaining immortality, or an extended replicative life span which leads to tumor progression in an organism. ❖ When DNA is damaged there is no way toarrest cell cycle at G1 phase and maintain damaged DNA. Damaged DNA results in loss of genetic information and mutations.
	NO	❖ Wild-type p16 inhibits binding of CDK4/6 with CycD by forming a complex p16CDK4/6, and thereby preventing Rb phosphorylation. ❖ If the reason of dysfunction is replicative senescence, cells enter in to a state of irreversible growth arrest. ❖ If the reason of dysfunction is DNAdamage, cell cycle is arrested at G1 phase until damaged DNA is maintained.	❖ CycD binds to CDK4/6 resulting in phosphorylation of Rb, causing successive cell division until Hayflick limit is reached in a healthy cell cycle state.

Fig. 2. Classification of biological events with respect to p16 mutation and G1-dysfunction.

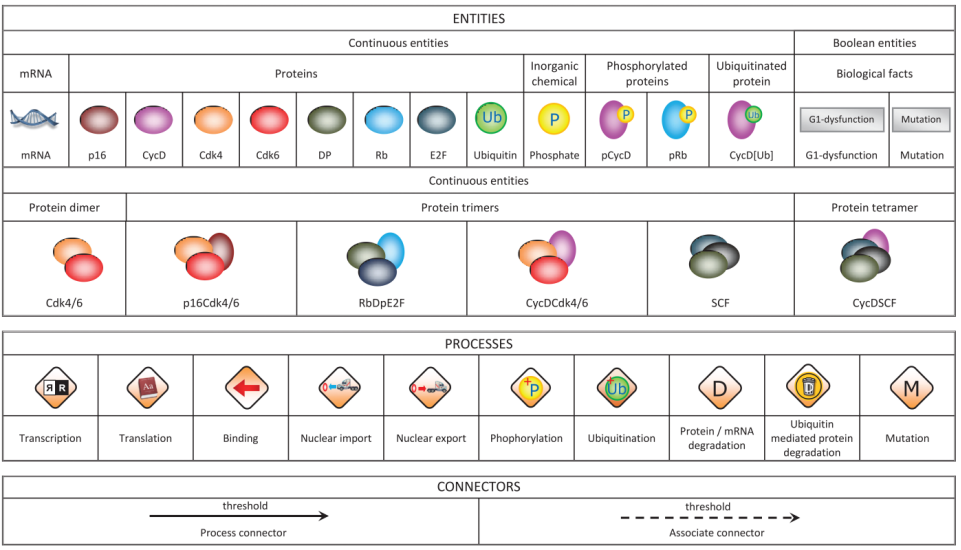

Fig. 3. The elements used in HFPN model.

interactions between major proteins, phosphorylation and proteasome-mediated ubiquitination.

HFPN model of p16-mediated pathway is composed of 28 continuous entities representing mRNAs, proteins, protein complexes, ubiquitin, phosphate, ubiquitinated and phosphorylated proteins; 2 generic entities indicating presence/absence of p16 mutation and G1-dysfunction; 44 continuous processes standing for transcription, translation, nuclear transport, binding, phosphorylation, ubiquitination, mRNA degradation, natural degradation and mutation; 74 process and associate connectors. The model comprises 30 variables **m1** to **m30**, two of which are introduced to indicate presence/absence status of p16 mutation (**m4**) and G1-dysfunction (**m6**), and remaining 28 variables are defined to measure the concentrations of biological components. The types and identifiers used in the present model are specified

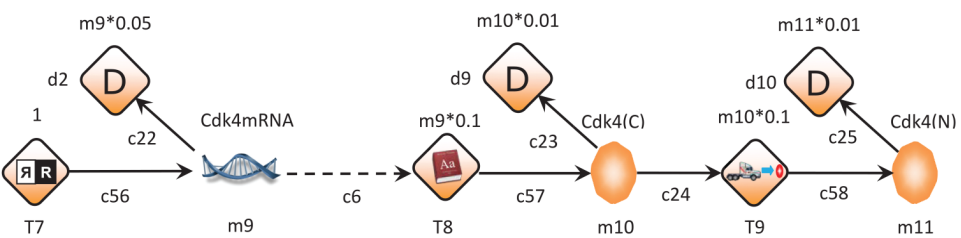

Fig. 4. Central dogma of biology illustrated for Cdk4: mRNA transcribed from DNA (T7) is then translated into protein (T8). Protein synthesized in cytoplasm is exported to nucleus (T9). Both mRNA and proteins undergo degradation (d2, d9 and d10).

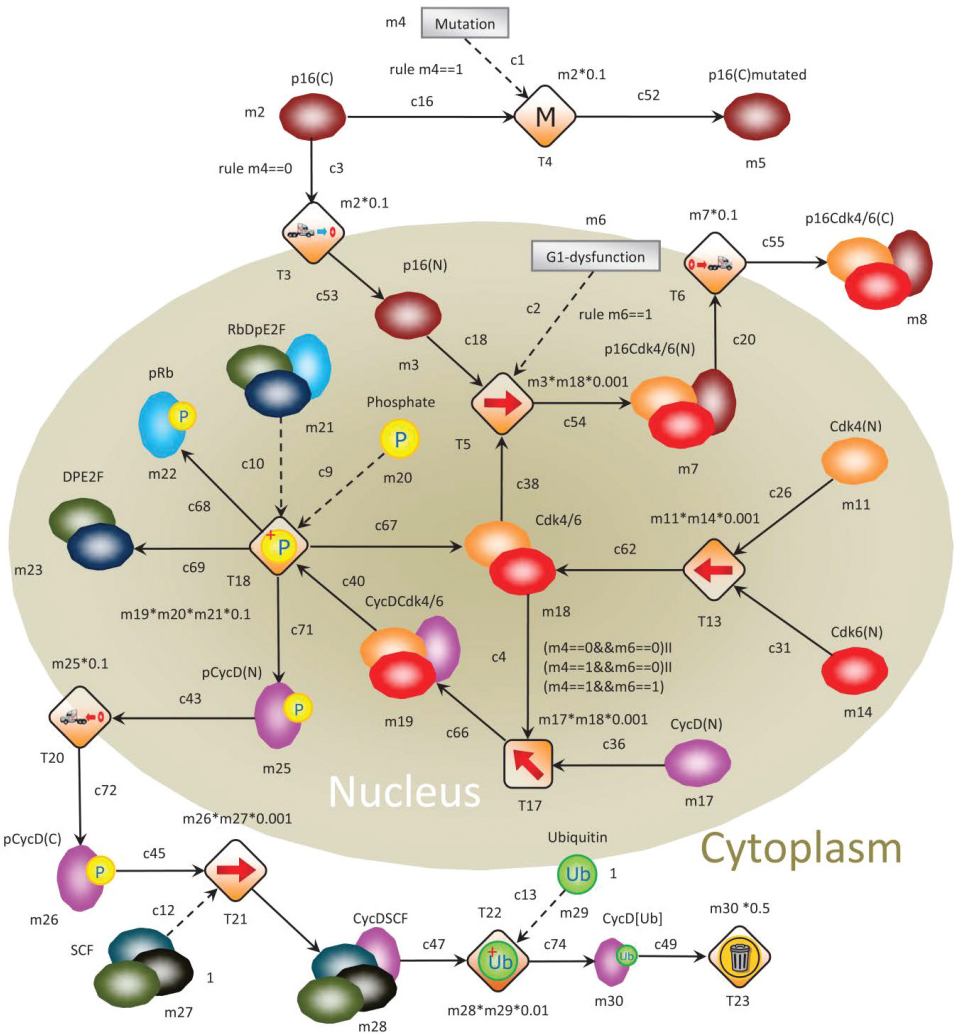

Fig. 5. HFPN representation of p16-mediated pathway in human cell cycle.

in Fig. 3. To keep the concentration of related mRNAs at specified level, we use associate connectors between mRNA entries and related transcription processes.

Relationship between entities and biological components is illustrated in Table 1. Likewise, correspondence between processes and biological phenomena is detailed in Tables 2 and 3. Information on connectors are described in Table 4. Given biological components X and Y, throughout the manuscript XmRNA, pX, X[Ub], X(N), X(C), Xmutated and XY stand for mRNA of X component, phosphorylated X component, ubiquitinated X component, nucleic, cytoplasmic, mutated concentrations of X component and complex of X and Y components, respectively.

Table 1. Correspondence between biological components and HFPN entities.

Entity name	Entity type	Variable	Initial value	Value type
p16mRNA	Continuous	m1	0	Double
p16(C)	Continuous	m2	0	Double
p16(N)	Continuous	m3	0	Double
Mutation	Generic	m4	True/false	Boolean
p16mutated	Continuous	m5	0	Double
G1-dysfunction	Generic	m6	True/false	Boolean
p16Cdk4/6(N)	Continuous	m7	0	Double
p16Cdk4/6(C)	Continuous	m8	0	Double
Cdk4mRNA	Continuous	m9	0	Double
Cdk4(C)	Continuous	m10	0	Double
Cdk4(N)	Continuous	m11	0	Double
Cdk6mRNA	Continuous	m12	0	Double
Cdk6(C)	Continuous	m13	0	Double
Cdk6(N)	Continuous	m14	0	Double
CycDmRNA	Continuous	m15	0	Double
CycD(C)	Continuous	m16	0	Double
CycD(N)	Continuous	m17	0	Double
Cdk4Cdk6	Continuous	m18	0	Double
CycDCdk4/6	Continuous	m19	0	Double
Phosphate	Continuous	m20	1	Double
RbDpE2F	Continuous	m21	1	Double
pRB	Continuous	m22	0	Double
DpE2F	Continuous	m23	0	Double
SPhaseGenes	Continuous	m24	0	Double
pCycD(N)	Continuous	m25	0	Double
pCycD(C)	Continuous	m26	0	Double
SCF	Continuous	m27	1	Double
CycDSCF	Continuous	m28	0	Double
Ubiquitin	Continuous	m29	1	Double
CycD[Ub]	Continuous	m30	0	Double

It is hard, if not impossible, to determine exact rates based on data coming from biological laboratory experiments. It is uncommon that two identical experiments lead to identical observations, since biological phenomenon depends on many parameters. The results of wet lab experiments regarding rate measurements may sometimes be contradictory. In this work, the rates of biological phenomena are estimated according to their relative rates. We first preset rate of transcription to 1, and then set the rates of remaining biological phenomena by comparing them with the rate of transcription. The process rates adopted in the present work are comparable to those in other works.[43,44] The process rates are presented in Table 2.

The elements of HFPN model are detailed in Fig. 3, while whole model is demonstrated in Fig. 5. A screen snapshot of HFPN model is illustrated in Fig. 6. The model allows rule-based processing of biological events in accordance with four scenarios mentioned in Fig. 2. Note that **T4** and **m4** control the status of **mutation**. Likewise, **G1-dysfunction** and **m6** check the presence of dysfunction in G1 phase. When p16 is mutated, the rule **m4==1** enables **T4**. Occurrence of **T4** arrests p16 in

Table 2. Correspondence between biological phenomena and HFPN processes.

Biological phenomenon	Process	Process type	Process rate
Transcription of p16mRNA	T1	Continuous	1
Translation of p16	T2	Continuous	m1*0.1
Nuclear import of p16	T3	Continuous	m2*0.1
Mutation of p16	T4	Continuous	m2*0.1
Binding of p16(N) and Cdk4/6	T5	Continuous	m3*m18*0.001
Nuclear export of p16Cdk4/6	T6	Continuous	m7*0.1
Transcription of Cdk4mRNA	T7	Continuous	1
Translation of Cdk4	T8	Continuous	m9*0.1
Nuclear import of Cdk4	T9	Continuous	m10*0.1
Transcription of Cdk6mRNA	T10	Continuous	1
Translation of Cdk6	T11	Continuous	m12*0.1
Nuclear import of Cdk6	T12	Continuous	m13*0.1
Binding of Cdk4 and Cdk6	T13	Continuous	m11*m14*0.001
Transcription of CycDmRNA	T14	Continuous	1
Translation of CycD	T15	Continuous	m15*0.1
Nuclear import of CycD	T16	Continuous	m16*0.1
Binding of Cdk4/6 and CycD	T17	Continuous	m17*m18*0.001
Phosphorylation of RB	T18	Continuous	m19*m20*m21*0.1
Transcription of S phase genes	T19	Continuous	m23*1
Nuclear export of pCycD	T20	Continuous	m25*0.1
Binding of pCycD and SCF	T21	Continuous	m26*m27*0.001
Ubiquitination of CycD	T22	Continuous	m28*m29*0.01
Degradation of CycD[Ub]	T23	Continuous	m30*0.5

Table 3. Natural degradations in the HFPN model.

Biological phenomenon	Process	Process type	Process rate
Degradation of mRNAs	d1–d4	Continuous	mi*0.05
Degradation of proteins	d5–d21	Continuous	mi*0.01

Table 4. Connectors in the HFPN model.

Connector	Firing style	Firing script	Connector type
c1	Rule	m4==1	Input association
c2	Rule	m6==1	Input association
c3	Rule	m4==0	Input process
c4	Rule	(m4==0 && m6==0) || (m4==1 && m6==0) || (m4==1 && m6==1)	Input process
c5–c13	Threshold	0	Input association
c14–c49	Threshold	0	Input process
c50–c74	Threshold	0	Output process

cytoplasm, indicating that p16 is no longer functional as an inhibitor. Otherwise, **T3** occurs in accordance with rule **m4==0**, transporting p16 from cytoplasm to nucleus. When dysfunction occurs in Gl phase, in appliance with rule **m6==1**, p16 inhibits formation of CycDCdk4/6 complex.

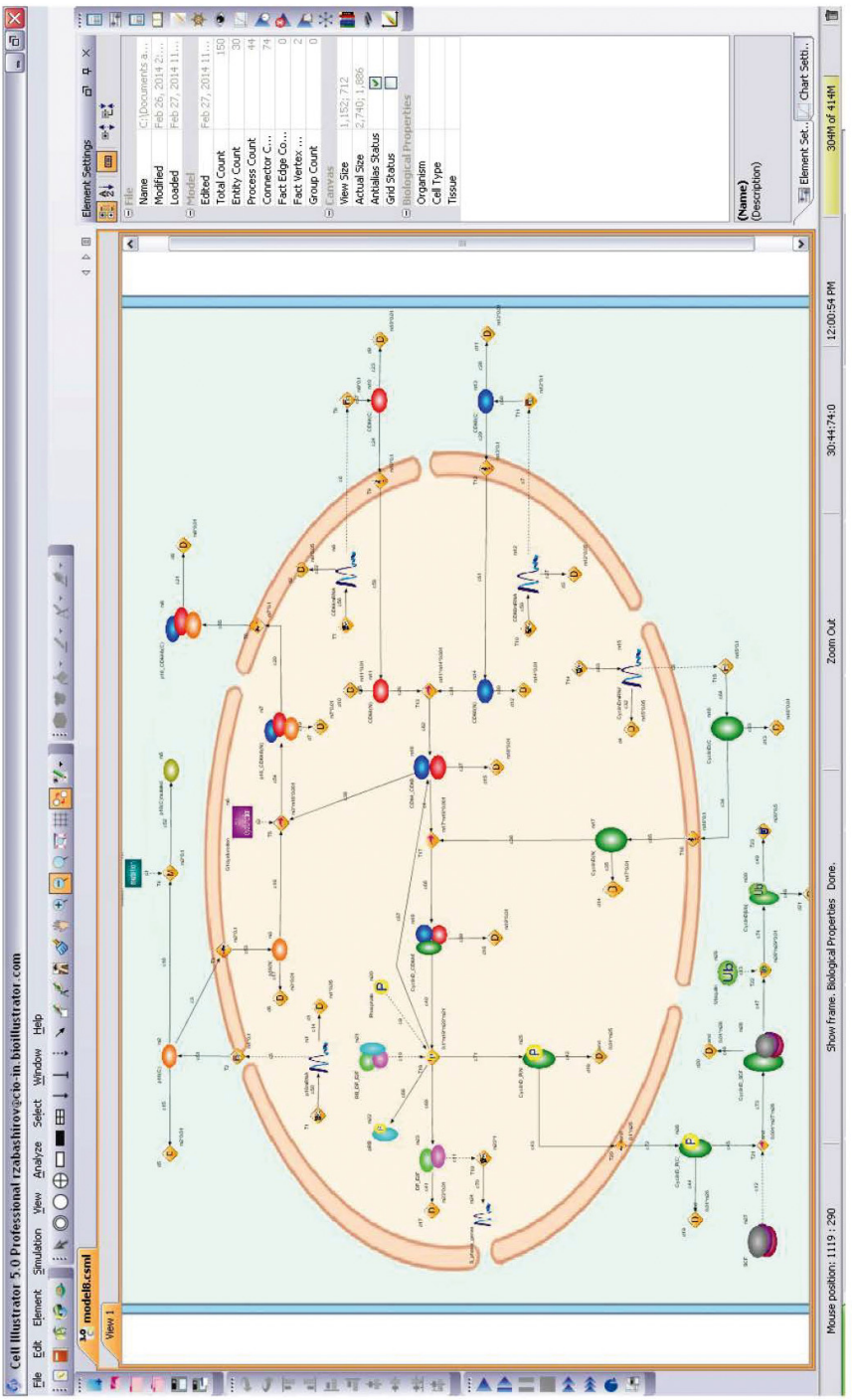

Fig. 6. Cell illustrator screen snapshot illustrating p16-mediated signalling pathway.

5. Simulations and Validation

The concentrations are plotted against time units called Petri time or pt, for short. In order to make simulation results comparable for all components, we performed the simulations at same pt sampling interval and consequently same simulation granularity. Although asymptotic behaviors of measured concentrations were observed within 200 pt, for clarity of observations we continued simulating until 500 pt. The simulations were conducted in accordance with the following four cases: (a) p16 is active but G1-dysfunction does not occur; (b) p16 is active and G1-dysfunction occurs; (c) p16 is inactivated and G1-dysfunction does not occur; and (d) p16 is inactivated and G1-dysfunction occurs.

Inactivation of p16 by the mutations has been reported to be a critical event in tumor progression. Almost 50% of all human cancers show loss of p16 function. There is evidence that some neoplasms exhibit remarkable amount of p16 concentration in cytoplasm. Study of cytoplasmic accumulation of p16 is indeed a recent event. The mechanisms behind p16 arrest in cytoplasm have not been clarified yet, though there are few hypotheses to explain the accumulation of p16 in cytoplasm. Simulation results in Fig. 7-I(c,d) reveal that inactivation of p16 is characterized by monotonic stable steady-state of p16 cytoplasmic concentration with approximately linear rate of growth. Close to the end of sampling time mutated p16 in cytoplasm reaches its peak level at 750. We know that p16 mutations usually arise in the form of promoter methylation, homozygotic deletion and loss of heterozygosity. Impact of mutation types to concentration behavior of p16 needs to be further investigated.

The consequences triggered by the loss of p16 function are indicated in Fig. 2. In the light of these scenarios, inactivation of p16 by the mutations arrests p16 in cytoplasm preventing its transportation to the nucleus. Nonexistence of p16 in nucleus causes p16 not to act as an inhibitor anymore. Even if DNA is damaged or Hayflick limit has reached, p16 is not able to bind to Cdk4/6. Since inhibitory mechanism does not work properly due to the mutation of p16, the formation of CycDCdk4/6 complex and phosphorylation of Rb cannot be stopped. Thus, the necessary cell cycle arrest cannot be realized by p16. As illustrated in Fig. 7(c,d) simulation results provide a good fit to aforesaid scenarios showing no accumulation of p16 in nucleus [Fig. 7-II(c,d)] and consequently no accumulation of p16Cdk4/6 in nucleus [Fig. 7-IV(c,d)] and in cytoplasm [Fig. 7-III(c,d)]. The simulation results in Fig. 7(c,d) do not show any difference no matter whether there is G1-dysfunction or not. This is an expected result as it is consistent with the aforementioned scenarios.

Some researchers report on complete disruption of cyclin D by proteasome-mediated ubiquitination at the end of G1 phase,[70] while others claim that unlike cyclins A, B and E, whose levels oscillate during the cell cycle, cyclin D is subsequently expressed throughout cell cycle, and its levels are more constant.[71–73] The majority of the researchers, on the other hand, suggest that in wild-type cells the cyclin D levels are high during G1 phase in response to growth factors to initiate DNA synthesis, but then it is suppressed to low levels during S phase to allow for efficient DNA synthesis,

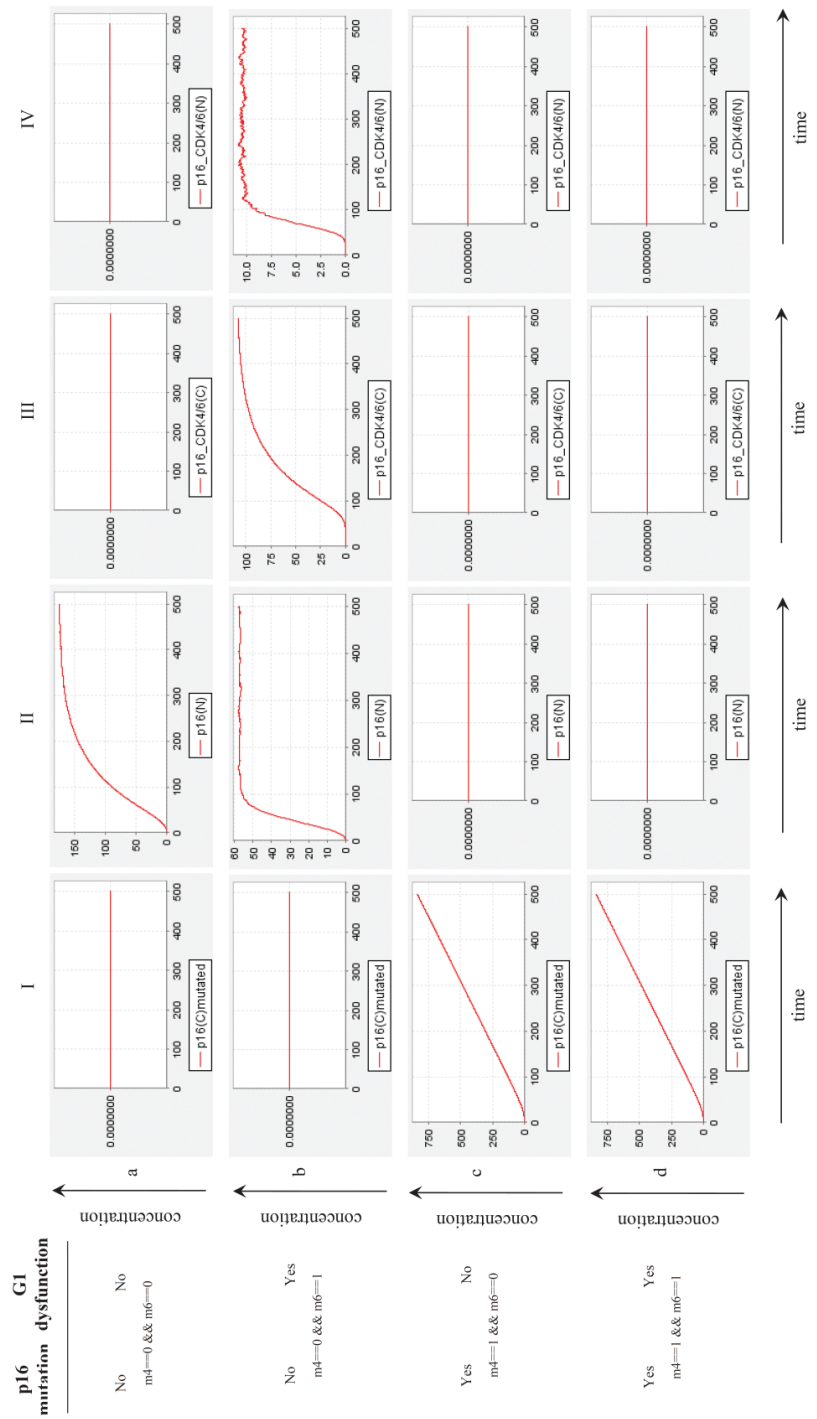

Fig. 7. Simulation results for p16(C)mutated, p16(N), p16_Cdk4-6(C) and p16_Cdk4-6(N).

and finally it is induced again in G2 phase to support proliferation.[74,75] There does not exist, however, absolute consensus among researchers regarding exact levels of cyclin D before, during and after the suppression.

Figure 9-III shows simulation results for concentration behavior of cyclin D in nucleus. As we observed, when p16 is inactivated by the mutations and/or dysfunction is not detected in G1 phase, the concentration of cyclin D within nucleus is induced rapidly so that it reaches the peak level at 50 in approximately 75 pt. Then the concentration is reduced rapidly to low levels due to the proteasome-mediated ubiquitination. Asymptotic behavior of cyclin D is clearly observed close to the concentration units of 175. Then cyclin D enters to the steady constant state. The simulation results in Fig. 9-III(a,c,d) show that the levels of cyclin D are high in G1 phase and it is low in the S phase, as it is observed by some researchers,[74,75] but it is neither completely disrupted as it is reported by other researchers[70] nor it is subsequently expressed to keep the concentration at constant level as it is suggested in several papers.[71–73]

When G1-dysfunction takes place, functional p16 inhibits binding of Cdk4/6 to cyclin D by forming the p16Cdk4/6 complex, preventing phosphorylation of Rb and consequently ubiquitination of cyclin D. This event might be predicted to result in accumulation of high levels of cyclin D concentration in nucleus. Simulation results illustrated in Fig. 9-III-b are in agreement with this prediction. The cyclin D concentration within sampling interval reaches its maximum level, which is close to 175 units. Furthermore, comparing the concentration levels of the p16Cdk4/6 in nucleus (Fig. 7-III-b) with cytoplasmic one (Fig. 7-IV-b) we observe that p16Cdk4/6 is mainly accumulated in cytoplasm rather than in nucleus. This result is rather interesting since to the best of our knowledge, this outcome has not been reported in the literature so far. Under assumption that p16 is functional at the absence of G1-dysfunction, cyclin D successfully binds to Cdk4/6 resulting in accumulation of functional p16 in nucleus (Fig. 7-II-a). Comparing two cases in Fig. 9-III-b and Fig. 7-II-a, we observe that maximum levels of cyclin D and p16 concentrations in the nucleus are the same, which is close to the level of 175 units.

It is broadly known that Cdk is an enzyme and therefore once produced, it is present throughout the cell cycle. It was also reported that Cdk levels remain relatively constant throughout the cell cycle.[49,65] Simulation results for Cdk4 and Cdk6 in Fig. 8 reveal that levels of Cdk proteins in cells vary little throughout the cell cycle, which is in agreement with the literature. The fact that equal amounts of cyclin D (Fig. 9-III-b) and p16 (Fig. 7-II-a) concentrations are available for binding with Cdk4/6 coupled with a constant rate of binding reaction might be predicted to result in equal amount of Cdk4/6 concentrations left after forming resulting complexes. However, simulation results for Cdk4/6 in Fig. 9-I is somewhat surprising — the amount of Cdk4/6 concentration remained is as high as 125 in cases (a), (c) and (d), and it is as low as 20 in case (b). The following could be a reasonable explanation for this observation. When DNA damage or replicative senescence takes place p16 binds to Cdk4/6 preventing Rb phosphorylation. This event consequently arrests cell cycle

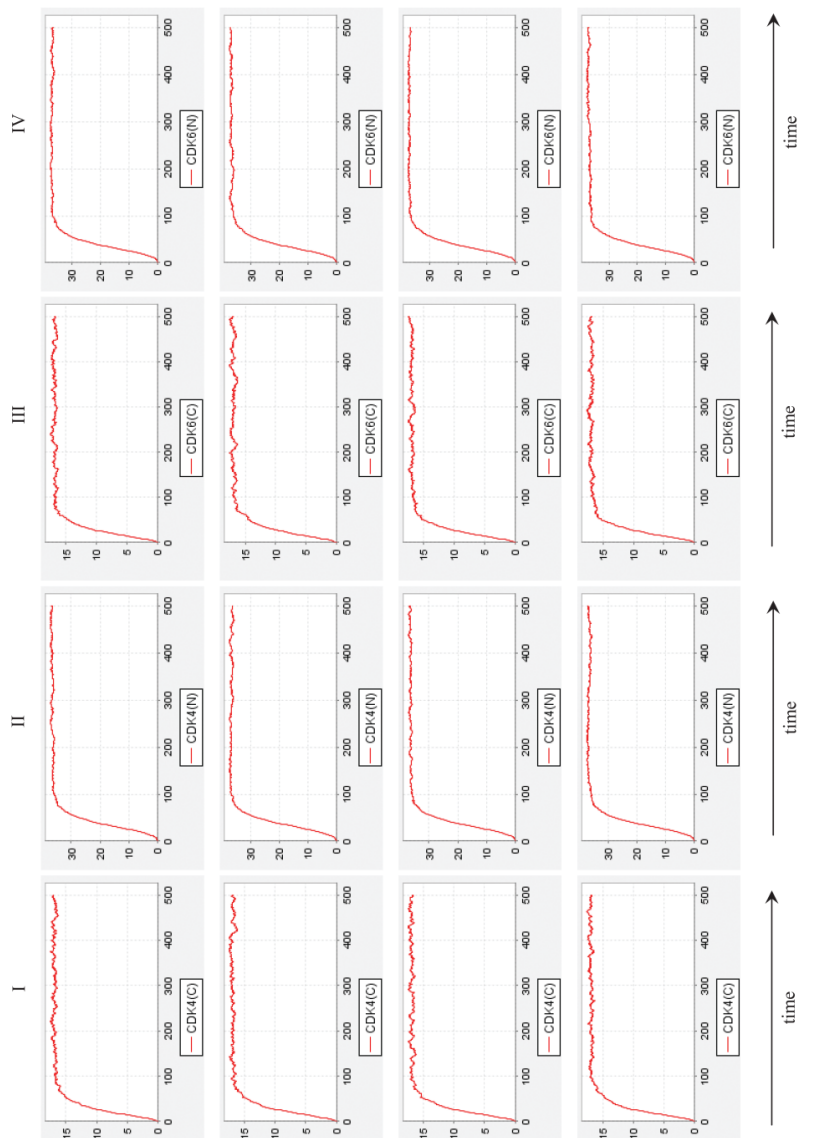

Fig. 8. Simulation results for Cdk4(C), Cdk4(N), Cdk6(C) and Cdk6(N).

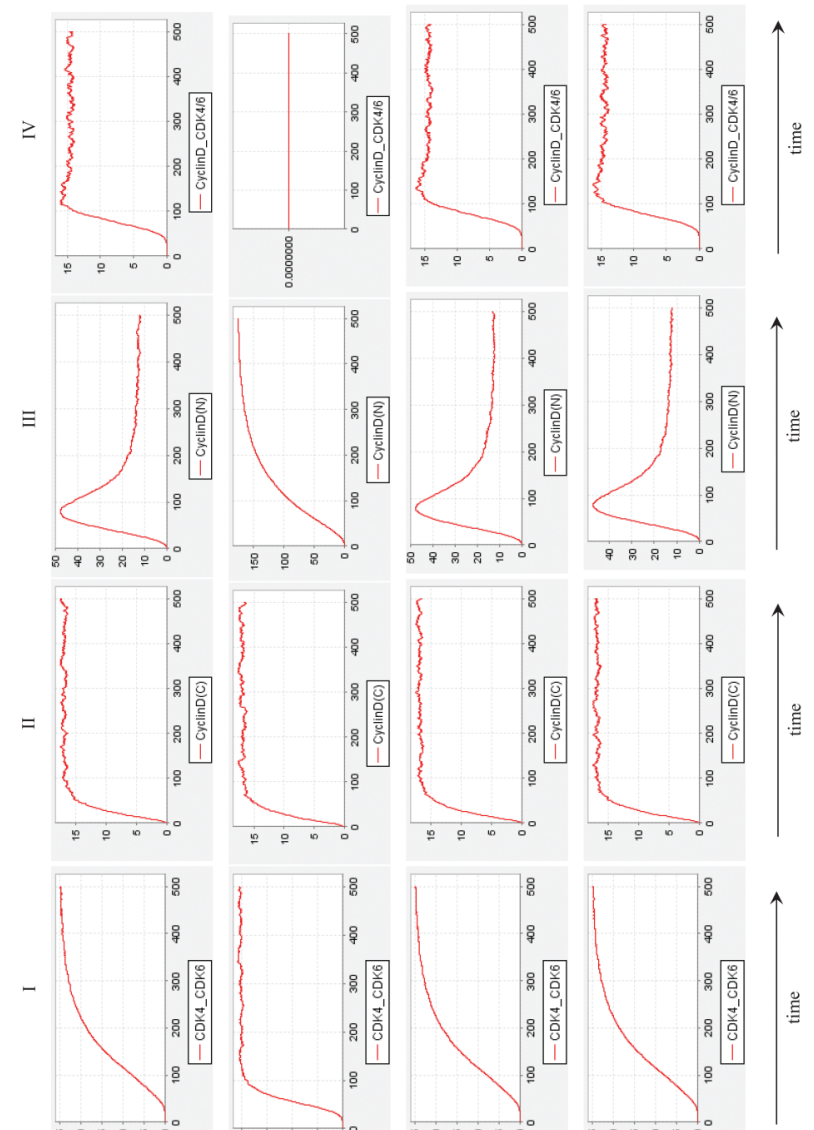

Fig. 9. Simulation results for Cdk4/6, CycD(C), CycD(N) and CycDCdk4-6.

until damaged DNA is maintained or it remains so continuously if replicative senescence occurs. Dynamic behavior of Cdk4/6 for case Fig. 9-I-b thus supports this idea as low levels of Cdk4/6 concentration remained after forming p16Cdk4/6 is insufficient to initiate Rb phosphorylation.

6. Concluding Remarks and Further Work

This paper describes detailed quantitative model of p16-mediated pathway in higher eukaryotes. Components of this pathway are frequently found to be inactivated, downregulated or overexpressed in human cancers. We perform simulations under assumptions regarding p16 inactivation by the mutations, DNA damage and replicative senescence. Simulation results show that our model is consistent with most of the available experimental observations about p16-mediated pathway. We are able to interpret the simulation results in a meaningful way whenever we fail to find an experimental observation to compare these results with.

The main findings of the present work are summarized below:

(a) Inactivation of p16 by the mutations, a critical event in tumor progression, results in an increase in its cytoplasmic concentration [Fig. 7-I(c,d)].
(b) In wild-type cells, the cyclin D levels are high during G1 phase to initiate DNA synthesis, but then it is suppressed to low levels during S phase to enable DNA synthesis (Fig. 9-III-a).
(c) When p16 is functional and there exists dysfunctionality in G1 phase, then p16Cdk4/6 is mainly accumulated in cytoplasm rather than in nucleus (Fig. 7-III-b, Fig. 7-IV-b).
(d) In wild-type cells, high levels of functional p16 is accumulated in the nucleus (Fig. 7-II-a).
(e) High levels of cyclin D are accumulated in nucleus when p16 is functional and DNA is damaged or replicative senescence occurs (Fig. 9-III-b).
(f) Simulation results for Cdk4 and Cdk6 reveal that levels of Cdk proteins in cells vary little throughout the cell cycle (Fig. 8).
(g) Cdk4/6 level is high in all cases [Fig. 9-I(a,c,d)] except when p16 is functional and DNA damage or replicative senescence occurs (Fig. 9-I-b). In the latter case, Cdk4/6 concentration is reduced to low levels, because functional p16 binds to Cdk4/6, causing nuclear export of resulting complex.

Our future goal and work in progress involves further elucidation of the available experimental data on this matter. In concert with experimental approaches, the next phase of our research will focus on developing analogously detailed model for p21-mediated pathway, G1-to-S and G2-to-M checkpoints. All these models can then be coupled to complete big picture of cell cycle in higher eukaryotes as a modular signaling network. The underlying dynamic behavior of these models might have implications in diagnosis, prognosis and treatment of human cancers.

Acknowledgment

We thank Hiroshi Matsuno for his help at early stages of this research and for his useful comments on this manuscript.

References

1. Nobori T *et al.*, Deletions of the cyclin-dependent kinase-4 inhibitor gene in multiple human cancers, *Nature* **368**(6473):753–756, 1994.
2. Stone S *et al.*, Complex structure and regulation of the p16 (MTS1) locus, *Cancer Res* **55**(14):2988–2994, 1995.
3. Rayess H, Wang MB, Srivatsan ES, Cellular senescence and tumor suppressor gene p16, *Int J Cancer* **130**(8):1715–1725, 2012.
4. Bracken AP *et al.*, The Polycomb group proteins bind throughout the INK4A-ARF locus and are disassociated in senescent cells, *Genes Dev* **21**(5):525–530, 2007.
5. Liu Y *et al.*, Expression of p16(INK4a) in peripheral blood T-cells is a biomarker of human aging, *Aging Cell* **8**(4):439–448, 2009.
6. Serrano M, Hannon GJ, Beach D, A new regulatory motif in cell-cycle control causing specific inhibition of cyclin D/CDK4, *Nature* **366**(6456):704–707, 1993.
7. Liggett WH, Sidransky D, Role of the p16 tumor suppressor gene in cancer, *J Clin Oncol* **16**(3):1197–1206, 1998.
8. Rocco JW, Sidransky D, p16(MTS-1/CDKN2/INK4a) in cancer progression, *Exp Cell Res* **264**(1):42–55, 2001.
9. Guejiofor KK *et al.*, The prognostic significance of the biomarker p16 in oropharyngeal squamous cell carcinoma, *Clin Oncol (R Coll Radiol)* **25**(11):630–638, 2013.
10. Dreyer JH *et al.*, Detection of HPV infection in head and neck squamous cell carcinoma: A practical proposal, *Virchows Arch* **462**(4):381–389, 2013.
11. Braunewell S, Bornholdt S, Superstability of the yeast cell cycle dynamics: Ensuring causality in the presence of biochemical stochasticity, *J Theor Biol* **245**:638–643, 2007.
12. Brazhnik P, Tyson JJ, Cell cycle control in bacteria and yeast: A case convergent evolution, *Cell Cycle* **5**:522–529, 2006.
13. Chen KC *et al.*, Kinetic analysis of a molecular model of the budding yeast cell cycle, *Mol Biol Cell* **11**:369–391, 2000.
14. Chen KC *et al.*, Integrative analysis of cell cycle control in budding yeast, *Mol Biol Cell* **15**:3841–3862, 2004.
15. Ciliberto A, Tyson JJ, Mathematical model for early development of the sea urchin embryo, *Bull Math Biol* **62**:37–59, 2000.
16. Csikasz-Nagy A *et al.*, Modeling the septation initiation network (SIN) in fission yeast cells, *Curr Genet* **51**:245–255, 2007.
17. Fujita S *et al.*, Modeling and simulation of fission yeast cell cycle on hybrid functional Petri net, *IEICE Trans Fundamentals* **E-87-A**(11):2919–2928, 2004.
18. Herajy M, Schwarick M, A hybrid Petri net model of the eukaryotic cell cycle, in *Proc 3rd Int Workshop on Biological Processes and Petri nets (BioPPN)*, Heiner M, Höfestaedt R (eds.), Vol. 852, CEUR, Hamburg, 25 June, pp. 29–43, 2012.
19. Li S *et al.*, A quantitative study of the cell division cycle of Cauloubacter crescentus stalked cells, *PLoS Comput Biol* **4**:e64, 2008.
20. Lygeros J *et al.*, Stochastic hybrid modeling of DNA replication across a complete genome, *Proc Natl Acad Sci USA* **105**:12295–12300, 2008.
21. Mura I, Csikasz-Nagy A, Stochastic Petri net extensions of a yeast cell cycle model, *J Theor Biol* **254**:850–860, 2008.

22. Novak B, Tyson JJ, Modeling the control of DNA replication in fission yeast, *Proc Natl Acad Sci USA* **94**:9147–9152, 1997.
23. Novak B, Tyson JJ, Numerical analysis of a comprehensive model of M-phase control in Xenopus oocyte extracts and intact embryos, *J Cell Sci* **106**(4):1153–1168, 1993.
24. Nurse PM, Cyclin dependent kinases and cell cycle control (Nobel Lecture), *Bioscience Rep* **22**(5–6):487–499, 2002.
25. Queralt E *et al.*, Downregulation of PP2A(Cdc55) phosphatase by separase initiates mitotic exit in budding yeast, *Cell* **125**:719–732, 2006.
26. Sriram K *et al.*, A minimal mathematical model combining several regulatory cycles from the budding yeast cell cycle, *IETSyst Biol* **1**:326–341, 2007.
27. Stelling J, Gilles ED, Mathematical modeling of complex regulatory networks, *IEEE Trans Nanobiosci.* **3**:172–179, 2004.
28. Steuer R, Effects of stochasticity in models of the cell cycle: From quantized cycle times to noise-induced oscillations, *J Theor Biol* **228**:293–301, 2004.
29. Sveiczer A *et al.*, Modeling the fission yeast cell cycle: Quantized cycle times in wee1-cdc25Delta mutant cells, *Proc Natl Acad Sci USA* **97**:7865–7870, 2000.
30. Csikasz-Nagy A, Computational systems biology of the cell cycle, *Brief Bioinform* **10**(4):424–434, 2009.
31. Fuß H, DW *et al.*, Mathematical models of cell cycle regulation, *Brief Bioinform* **6**(2):163–177, 2005.
32. Csikasz-Nagy A, Computational systems biology of the cell cycle, *Brief Bioinform* **10**(4):424–434, 2009.
33. Stevaux O, Dyson NJ, A revised picture of the E2F transcriptional network and RB function, *Curr Opin Cell Biol* **14**:684–691, 2002.
34. Trimarchi JM, Lees JA, Sibling rivalry in the E2F family, *Nat Rev Mol Cell Biol* **3**:11–20, 2002.
35. Hayflick L, The limited in vitro lifetime of human diploid cell strains, *Exp Cell Res* **37**:614–636, 1965.
36. Matheu A *et al.*, Anti-aging activity of the Ink4/Arf locus, *Aging Cell* **8**(2):152–161, 2009.
37. Walkley CR, Orkin SH, RB is dispensable for self-renewal and multilineage differentiation of adult hematopoietic stem cells, *Proc Natl Acad Sci USA* **103**(24):9057–9062, 2006.
38. Baker DJ *et al.*, Opposing roles for p16Ink4a and p19Arf in senescence and ageing caused by BubR1 insufficiency, *Nat Cell Biol* **10**(7):825–836, 2008.
39. David R, Alla H, Continuous Petri nets, *Proc. 8th European Workshop on Application and Theory of Petri nets*, Zaragosa, Spain, pp. 275–294, 1987.
40. Alla H, David R, Continuous and hybrid Petri nets, *J Circuits Syst Comput* **8**(1):159–188, 1998.
41. Li S *et al.*, Simulation-based model checking approach to cell fate specification during Caenorhabditis elegans vulval development by hybrid functional Petri net with extension, *BMC Syst Biol* **3**(42), 2009.
42. Matsuno H *et al.*, Biopathways representation and simulation on Hybrid Functional Petri Nets, *In Silico Biol* **3**(3):389–404, 2003.
43. Doi A *et al.*, Constructing biological pathway models with Hybrid Functional Petri Nets, *In Silico Biol* **4**(3):271–291, 2004.
44. Doi A *et al.*, Simulation-based validation of the p53 transcriptional activity with hybrid functional Petri net, *In Silico Biol* **6**(1–2):1–13, 2006.
45. Weinert T, Hartwell L, Control of G2 delay by the rad9 gene of Saccharomyces cerevisiae, *J Cell Sci Suppl* **12**:145–148, 1989.
46. Pomerening JR *et al.*, Building a cell cycle oscillator: Hysteresis and bistability in the activation of Cdc2, *Nat Cell Biol* **5**:346–351, 2003.

47. Sha W *et al.*, Hysteresis drives cell-cycle transitions in Xenopus laevis egg extracts, *Proc Natl Acad Sci USA* **100**:975–980, 2003.
48. Cross FR *et al.*, Testing a mathematical model for the yeast cell cycle, *Mol Biol Cell* **13**:52–70, 2002.
49. Morgan DO, Principles of CDK regulation, *Nature* **374**:131–133, 1995.
50. Calzone L *et al.*, Dynamical modeling of syncytial mitotic cycles in Drosophila embryos, *Mol Syst Biol* **3**:131, 2007.
51. Gerard C, Goldbeter A, Temporal selforganization of the cyclin/Cdk network driving the mammalian cell cycle, *Proc Natl Acad Sci USA* **106**(21):21643–21648, 2009.
52. Swat M *et al.*, Bifurcation analysis of the regulatory modules of the mammalian G1-S transition, *Bioinformatics* **20**(10):1506–1511, 2004.
53. Qu Z *et al.*, Regulation of the mammalian cell cycle: A model of the G1-to-S transition, *Am J Physiol Cell Physiol* **254**:344–364, 2013.
54. Szallasi Z *et al.*, System Modeling in Cellular Biology: From Concepts to Nuts and Bolts, MIT Press, Cambridge, MA, 2006.
55. Chaouiya C, Petri net modelling of biological networks, *Brief Bioinform* **8**:210–219, 2007.
56. Assaraf YG *et al.*, Computer modelling of antifolaten, inhibition of folate metabolism using hybrid functional petri nets, *J Theor Biol* **240**:637–647, 2006.
57. Castellini A *et al.*, Hybrid functional Petri nets as MP systems, *Nat Comput* **9**(1):61–81, 2010.
58. Kaufmann K *et al.*, Modelling the molecular interactions in the flower developmental network of Arabidopsis thaliana, *Ann Botany* **107**(9):1545–1556, 2011.
59. Çetin N, Bashirov R, Tüzmen Ş, Petri net based modelling and simulation of p16-Cdk4/6-Rb pathway, in *Proc 4th Int Workshop on Biological Processes and Petri nets (BioPPN)*, Heiner M, Balbo G (eds.), Vol. 988, CEUR, Milan, 24–25 June 2013, pp. 30–44, 2013.
60. Nagasaki M *et al.*, Genomic object net: A platform for modelling and simulating biopathways, *Appl Bioinformatics* **2**(3):181–184, 2004.
61. Dori-Bachash M *et al.*, Coupled evolution of transcription and mRNA degradation, *PLoS Biol* **9**(7):e1001106, 2011.
62. Agherbi H *et al.*, Polycomb mediated epigenetic silencing and replication timing at the INK4a/ARF locus during senescence, *PLoS One* **4**(5):e5622, 2009.
63. Bartkova J *et al.*, The p16-cyclinD/Cdk4-pRb pathway as a functional unit frequently altered in melanoma pathogenesis, *Cancer Res* **56**(23):5475–5483, 1996.
64. Lin DI *et al.*, Phosphorylation-dependent ubiquitination of cyclin D1 by the SCF(FBX4-alphaB crystallin) complex, *Mol Cell* **24**(3):355–366, 2006.
65. Malumbres M, BaRbacid M, Cell cycle, Cdks and cancer: A changing paradigm, *Nat Rev Cancer* **9**(3):153–166, 2009.
66. Murray AW, Recycling the cell cycle: Cyclins revisited, *Cell* **116**:221–234, 2004.
67. Sherr CJ, Cancer cell cycle, *Science* **274**:1672–1677, 1996.
68. Vidal A, Koff A, Cell-cycle inhibitors: Three families united by a common cause, *Gene* **247**(1–2):1–15, 2000.
69. Weissman AM *et al.*, The predator becomes the prey: Regulating the ubiquitin system by ubiquitylation and degradation, *Nat Rev Mol Cell Biol* **12**(9):605–620, 2011.
70. Moeller SJ, Sheaff RJ, G1 phase: Components, conundrums, context, in *Cell Cycle Regulation*, Kaldis P (ed.), Springer-Verlag, Berlin, Heidelberg, 2005.
71. Bird RC, Role of cyclins and cyclin-dependent kinases in G1 phase prpgression, in *G1 Phase Progression*, Boonstra J (ed.), Kluwer Academic, New York, pp. 40–57, 2003.
72. Boonstra J, Restriction points to the G1 phase to the mammalian cell cycle, in *G1 Phase Progression*, Boonstra J (ed.), Kluwer Academic, New York, pp. 1–7, 2003.

73. Post SM, Lee E, Detection of kinase and phosphatase activities, *Methods Mol Biol* **241**:285–297, 2004.
74. Yang K *et al.*, Variations in cyclin D1 levels through the cell cycle proliferative fate of a cell, *Cell Division* **1**(32), 2006, doi: 10.1186/1747-1028-1-32.
75. Stacey DW, Three observations that have changed our understanding of cyclin D1 and p27 in cell cycle control, *Genes and Cancer* **12**(1):1189–1199, 2010.

Nimet İlke Akçay received her B.Sc. degree in Mathematics from İzmir University of Economics and M.Sc. degree in Biomathematics from Illinois State University in 2009 and 2011, respectively. She is currently a Ph.D. Candidate and Research Assistant in Eastern Mediterranean University, North Cyprus. Her research areas include Bioinformatics, Petri Nets and Mathematical Modeling.

Rza Bashirov received his B.Sc. degree in Applied Mathematics from Baku State University and his Ph.D. degree in Computer Science from Moscow State University in 1982 and 1990, respectively. He is currently Dean of the Faculty of Arts and Sciences and Professor in Eastern Mediterranean University, North Cyprus. His current research interests include Bioinformatics, Petri Nets and Cryptography.

Şükrü Tüzmen received his B.Sc., M.Sc. degrees in Biology and Ph.D. degree in Molecular Biology and Genetics from Boğaziçi University, İstanbul, in 1990, 1992 and 1995, respectively. He is currently Associate Professor at the Eastern Mediterranean University, North Cyprus. He also holds adjunct positions at the Translational Genomics Research Institute, Arizona State University, and the University of Maryland University College. His current research interests include advancing the molecular genetics of human genome by studying the associations between drugs, genes, pathways and diseases.